Int. J. Electrochem. Sci., 16 **(2021)** 150653, doi: 10.20964/2021.01.61

International Journal of
ELECTROCHEMICAL
SCIENCE
www.electrochemsci.org

Synthesis of Activated Carbon Derived from Garlic Peel and Its Electrochemical Properties

Tongtong Ji, Kuihua Han[*]*, Zhaocai Teng, Jinxiao Li, Meimei Wang, Jigang Zhang,*
Yang Cao, Jianhui Qi

Shandong Engineering Laboratory for High-efficiency Energy Conservation and Energy Storage
Technology & Equipment, School of Energy and Power Engineering, Shandong University,
Jinan 250061, shandong, China
[*]E-mail: hankh@163.com

Received: 15 June 2020 / *Accepted:* 30 October 2020 / *Published:* 30 November 2020

In this paper, hydrochloric acid pretreatment process was used to fabricate the garlic peel-based activated carbon (HGAP) with garlic peel as carbon precursor and KOH as an activator. The single factor experiment method was used to explore the effects of hydrochloric acid concentration, treatment time, water bath temperature, and carbonization temperature on the pore structure of garlic-based activated carbon. Nitrogen adsorption and desorption, XRD, Raman spectroscopy, constant current charge and discharge, cyclic voltammetry and other characterization methods were used to characterize the physical morphology and electrochemical performance of garlic peel-based activated carbon. The results show that the optimal process conditions for preparing the HGAPs are as follows: heating and stirring in a water bath with 1.0 mol/L hydrochloric acid solution at 60℃ for 3 h, and the carbonization temperature is 600℃.The specific surface area of HGAP-7 synthesized under the optimal conditions is as high as 3325.2 $m\,g^{-1}$, and the pore volume is 1.881 $cm^3\,g^{-1}$. Using 6 M KOH as electrolyte, the supercapacitor assembled by HGAP-7 has a specific capacitance of 424.42 $F\,g^{-1}$ at a current density of 1 $A\,g^{-1}$. Compared with non-pretreated garlic peel-based activated carbon, the mesopore contents of HGAPs significantly increase, and the cycle characteristics and rate performance of the supercapacitors are improved.

Keywords: hydrochloric acid pretreatment; garlic peel; activated carbon; supercapacitor

1. INTRODUCTION

As an electrochemical energy storage device with excellent performance[1-3], supercapacitor has become the current research hotspot because of its advantages of high power density, long storage life, wide operating temperature range, short charging time and long cycle life[4,5]. The supercapacitor is composed of electrode materials, current collectors, electrolytes, and separators[6,7]. Especially, the electrode material is a key factor to capacitor electrochemical performance[8]. Biomass-based activated carbon has become the most popular commercial electrode material due to its low cost, easy accessibility and natural pore structure[9,10]. At present, fabricating activated carbon with a high specific surface area and a high mesopore content is an efficient method to improve the energy density and the power density of the supercapacitors[11].

Commonly, metal oxides or salts which are composed of K, Ca, Na, Mg and other metal elements exist inside the biomass [12-14], and they have great impact on biomass pyrolysis[15,16]. On the one hand, it is conducive to the formation of coke and gas products; on the other hand, it will reduce the stability of the carbon skeleton[17]. Sun and other research scholar have found that the wood tar generated from biomass pyrolysis has a strong catalytic effect on pyrolysis process, which is considered to be caused by inorganic minerals such as alkali metals contained in wood tar[18]. Therefore, exploring the effect of endogenous minerals existed in biomass on the carbon skeleton and its electrochemical performance of biomass-based activated carbon is of great significance.

Using garlic peel as the carbon precursor, Zhang synthesized garlic skin-derived 3D hierarchical porous carbon with high specific surface area by a simple KOH activation method[19], proving that garlic peel is a high-quality raw material for preparing activated carbon. In this study, garlic peel from Jinxiang, Shandong Province was selected as the experimental material, and hydrochloric acid pretreatment process was used to remove Ca, Mg, K and other endogenous minerals contained in garlic peel[20].Moreover, KOH was used as an activator to prepare garlic peel-based activated carbon. At the same time, nitrogen adsorption and desorption, XRD, Raman spectroscopy, constant current charge and discharge, cyclic voltammetry and other characterization methods were used for analyzing the pore structure, graphitization degree and electrochemical performance of garlic peel-based activated carbon.

2. EXPERIMENTAL

2.1 Preparation of garlic peel -based activated carbon

In this study, garlic peel was selected as the carbon precursor, and it was obtained from Jinxiang, Shandong province. The garlic peel was dried in a blast drying oven at 105°C for 24 h, then crushed with a grinder for 3 min, and sieved with an 80 mesh sieve to obtain garlic peel powder with a diameter of less than 180 um. Table 1 is the number of samples under different experimental conditions.

The preparation of activated carbon includes the following four steps: hydrochloric acid pretreatment, carbonization, activation, washing and purification. The experimental steps of hydrochloric acid pretreatment are as follows: setting the range of water bath temperature (20-80°C), placing garlic peel and hydrochloric acid solutions of different concentrations (0.5-2.0 mol L^{-1}) in a beaker according to a ratio of 1: 50 g mL^{-1}. The time set in the stirring experiment (1-7 h), after the water bath stirring was completed, wash it to neutral with deionized water, and carbonized after drying. The procedures of carbonization are as follows: taking 20 g pretreated garlic peel into a tube furnace at the temperature of 400 to 700°C for 2 hours. At the same time, high-purity nitrogen (purity $\geq$99.999%) was used as the protective gas. The procedures of activation were as follows: KOH and carbonized garlic peel powder were immersed at a ratio of 4: 1, then a small amount of deionized water was added to prepare a mixture, finally immersed in a blast drying oven at 80℃ for 2 h. The carbonized product after impregnation was placed in an atmosphere muffle furnace with high-purity nitrogen as the protective gas. The carbon was activated at the temperature of 350℃ for 0.5 h, then at the temperature of 800℃ for 2 h. During the whole process of carbonization and activation, the heating rate was 5 ℃ min^{-1}, and the protective gas flow rate was 1 L min^{-1}. The procedures of washing and purification were as follows: the activated carbon was placed in a thermostatic water bath at 80℃ with magnetic stirring for 30 min, and then washed with deionized water until neutral. Add an appropriate amount of 1.0 mol L^{-1} hydrochloric acid dropwise to PH=2, stir magnetically in a water bath at 80℃ for 30 min, and wash repeatedly with deionized water until neutral, put it in a blast drying oven at 105℃ and dry for 24 h. The garlic peel-based activated carbon samples were separately numbered as HGAP-n. The compared sample GAP was prepared without hydrochloric acid pretreatment experiment, and the carbonization temperature was 600℃. The rest of the experimental conditions were the same with HGAP-n.

Table 1. The number of samples under different experimental conditions

Experimental variable	Sample serial number	Tretment time(h)	Water bath temperature(℃)	Hydrochloric acid concentration(mol/L)	Carbonization temperature(℃)
Treatment time	HGAP-1	1	80	1.0	600
	HGAP-2	3	80	1.0	600
	HGAP-3	5	80	1.0	600
	HGAP-4	7	80	1.0	600
Water bath temperature	HGAP-5	3	20	1.0	600
	HGAP-6	3	40	1.0	600
	HGAP-7	3	60	1.0	600
Hydrochloric acid concentration	HGAP-8	3	60	0.5	600
	HGAP-9	3	60	1.5	600
	HGAP-10	3	60	2.0	600
Carbonization temperature	HGAP-11	3	60	1.0	400
	HGAP-12	3	60	1.0	500
	HGAP-13	3	60	1.0	700
\	GAP	\	\	\	600

2.2 Electrochemical measurement

The HGAP-7 sample with the largest specific surface area and the non-pretreated control sample GAP were selected as active material of electrodes to assemble supercapacitors. The activated carbon, conductive graphite and polytetrafluoroethylene emulsion (PTFE, 60 wt%) were mixed according to a mass ratio of 8: 1: 1, then 25 ml absolute ethanol was added for making the mixture. The mixture was treated by ultrasonic dispersion for 30 min . After the treatment, the mixture was dried in a blast drying oven at 80℃. Then the mixture was evenly spread on a foam nickel with a diameter of 1.5 cm and dried it in a vacuum oven at 80℃ for 12 h. After that , it was pressed at 14 MPa for 1 min. The prepared electrode sheets and aqueous separators were immersed in 6 mol L^{-1} KOH solution for 2 h to be assembled the button supercapacitors. The assembly sequence was as follows: positive electrode-gasket-electrode-separator-electrode-negative.

2.3 Characterization of activated carbon

Nitrogen adsorption and desorption isotherms were obtained by specific surface area and pore size distribution analyzer (JW-BK132F). The specific surface area of activated carbon was calculated by Brunauer-Emmett-Teller (BET) method, and the Barrett-Joyner-Halenda (BJH) method was used for calculating the pore volume and pore size distribution. The surface morphology and surface element distribution of the activated carbon were observed with a scanning electron microscope (SUPRATM 55) equipped with EDS.X-ray diffractometer (D/MAX-2500PC) was used to determine the graphite crystallite structure of the samples. The electrochemical performance tests of the supercapacitors were carried out by the electrochemical workstation (CHI600E).

3. RESULTS AND DISCUSSION

3.1 Effects of synthesis conditions on pore structure of garlic peel-based activated carbon

3.1.1 Effect of water bath time on specific surface area

The water bath temperature was kept at 80°C, hydrochloric acid concentration 1.0 mol/L, and carbonization temperature 600°C, the effect of treatment time on the specific surface area of garlic peel-based activated carbon was explored. As can be seen from Figure 1 (a), as the bath time increases, the specific surface area increases first and then decreases, the specific surface area reaches its maximum at 3 h. When the treatment time is too long, the original tissue structure of garlic peel was destroyed by etching with hydrochloric acid solution. In the subsequent high-temperature carbonization activation, the original structure of garlic peel is prone to collapse, cannot continue to form pores, resulting in a decrease in specific surface area.

3.1.2 Effect of water bath temperature on specific surface area

Under the experimental conditions of treatment time of 3 h, hydrochloric acid concentration of 1.0 mol/L, and carbonization temperature of 600°C, the effect of water bath temperature on the specific surface area of garlic peel-based activated carbon was explored. It can be inferred from Figure 1 (b), When the pretreatment temperature is too low, hydrochloric acid cannot effectively remove impurities contained in garlic peel. When the temperature is greater than 60°C, the specific surface area is significantly increased. It shows that the higher pretreatment temperature is beneficial to the reaction of hydrochloric acid solution with impurities and endogenous minerals in garlic peel. The garlic peel after demineralization can form a more excellent pore structure in the subsequent carbonization activation process.

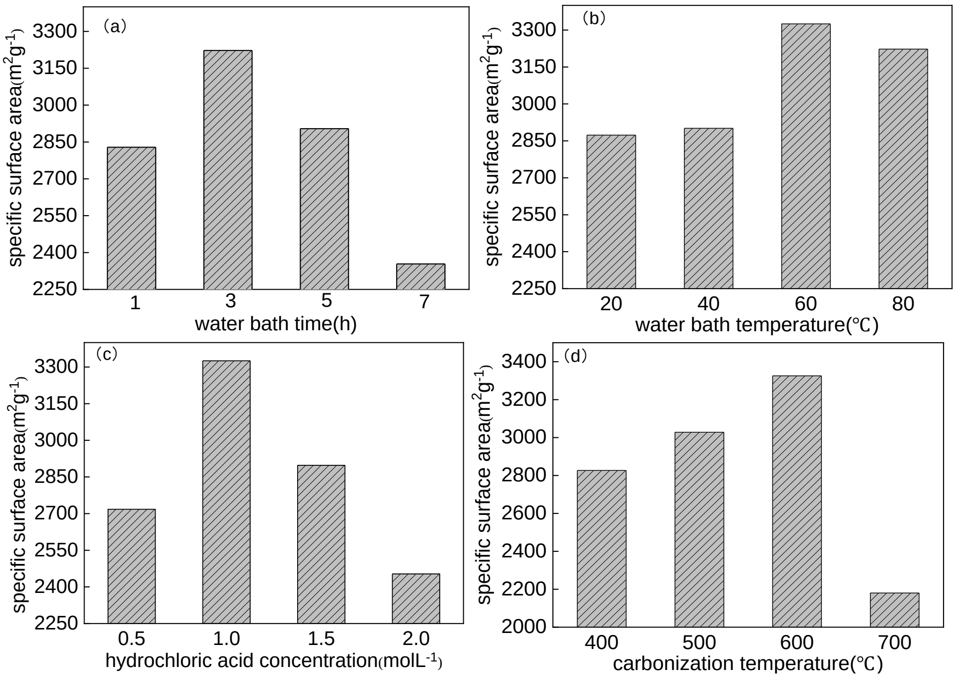

Figure 1. Effect of synthetic conditions on specific surface area (a) treatment time; (b) water bath temperature; (c) hydrochloric acid concentration; (d) carbonization temperature

3.1.3 Effect of hydrochloric acid concentration on specific surface area

The treatment time was kept for 3 h at the temperature of 60°C, and carbonization temperature was 600°C, the effect of hydrochloric acid concentration on the specific surface area of garlic peel based activated carbon was investigated As can be seen from Figure 1 (c), changing the concentration of hydrochloric acid has great effect on the specific surface area of activated carbon. When the concentration of hydrochloric acid is 0.5 mol L^{-1}, Hydrochloric acid cannot react with endogenous minerals sufficiently. However, when the hydrochloric acid concentration exceeds 1.0 mol L^{-1}, the specific surface area decreases significantly. When the hydrochloric acid concentration is 2.0 mol L^{-1}, the specific surface area is only 2452.9 m^2 g^{-1}. It proves that when the concentration of hydrochloric acid is too high, it will destroy the original natural structure of garlic peel. According to the picture, the content of pore structure that can be formed by garlic peel itself during the subsequent carbonization pore structure content reduced, and the specific surface area is decreased.

3.1.4 Effect of carbonization temperature on specific surface area

Endogenous minerals have a catalytic effect on biomass pyrolysis, in order to obtain high specific surface area activated carbon, continue to explore the optimal carbonization temperature of garlic peel after demineralization. At this time, the experimental conditions were treatment time 3 h, water bath temperature 60°C, hydrochloric acid concentration 1.0 mol/L. As can be seen from Figure 1 (d), when the carbonization temperature rises from 400°C to 600°C, the specific surface area reaches the maximum. The reason is that this carbonization temperature can provide enough energy to fully pyrolyze the garlic peel, evaporating most of the non-carbon components is conducive to the formation of initial pores. When the temperature rises to 700℃, the specific surface area of garlic peel-based activated carbon drops sharply, only 2180.3 m^2/g. Explain that too high temperature will destroy the mechanical strength of the initial pores of garlic peel. As a result, the formed pores collapse in the subsequent activation process, and the specific surface area decreases.

In summary, the process of pickling pretreatment of the sample with the largest specific surface area HGAP-7 is as follows: treatment time 3 h, water bath temperature 60℃, hydrochloric acid concentration 1.0 mol/L, carbonization temperature 600℃.

3.2 Characterization of garlic peel-based activated carbon

3.2.1 Pore structure of garlic peel-based activated carbon

In order to better compare the pore structure of activated carbon, groups 2, 4, 7, 13 and non-pretreated garlic peel-based activated carbon GAP were selected for nitrogen adsorption-desorption and pore size distribution characterization. As can be seen from Figure 2, the nitrogen adsorption-desorption curves of the five groups of garlic peel-based activated carbon are all typical IV type. When the relative pressure is less than 0.01, it is mainly the micropores of activated carbon for N_2 adsorption. At this time, the isothermal adsorption curves of the five groups of garlic peel-based activated carbon all rose sharply, indicating that the five garlic peel-based activated carbon samples contained a large number of microporous structures[21]. With the relative pressure rising to the stage of 0.5-1.0, the adsorption-desorption curves show the characteristics of rising tail and hysteresis ring, indicating that all five samples have a certain amount of mesopores[22].

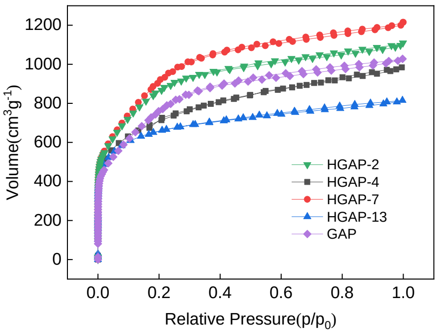

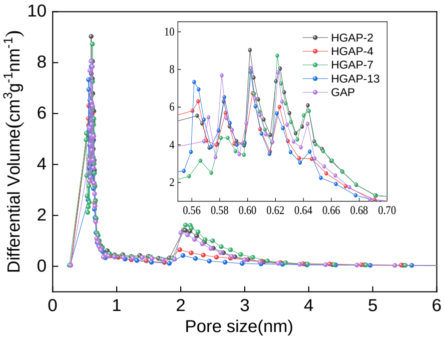

Figure 2. N_2 adsorption-desorption curve of garlic-based activated carbon Figure 3 Pore size distribution curves of garlic-based activated carbon

And the adsorption capacity of HGAP-7 with higher specific surface area is much higher than GAP and other samples. It can be seen from Figure 3 that the pore sizes of the five activated carbon samples are distributed between 0-6 nm, micropores are mainly at 0-1 nm and mesopores are mainly at 2-3 nm. It can be seen that the mesopore content of HGAP-7 is significantly more than other samples, indicating that although the hydrochloric acid pretreatment did not change the pore size range of the mesopores, it greatly increased the number of mesopores. Mesopores can effectively shorten the transmission distance for the ions, the increase in mesopore content is conducive to the transport of electrolyte ions and the improvement of electrochemical performance[23], hydrochloric acid pretreatment also increased the specific surface area and mesopore content of garlic peel-based activated carbon HGAP-7, which was beneficial to the improvement of electrochemical performance.

3.2.2 Scanning electron microscope analysis

Fig. 4 is the scanning electron micrograph of the original garlic peel, the original garlic peel after pickling with the best process, and the garlic peel-based activated carbon HGAP-7 magnified 20,000 times and 50,000 times. It is obvious from a and b that hydrochloric acid pre-pickling can wash away surface impurities and make the surface of garlic peel clear. This facilitates the production of subsequent pore structures. As can be seen from c and d, HGAP-7 has the characteristics of loose and porous, the pore structure is mostly round. When transporting electrolyte ions into activated carbon, round pores have better ion transmission efficiency than irregular pore structures such as cracks. It can reduce the resistance of ion transportation and is suitable as the electrode material for supercapacitors.

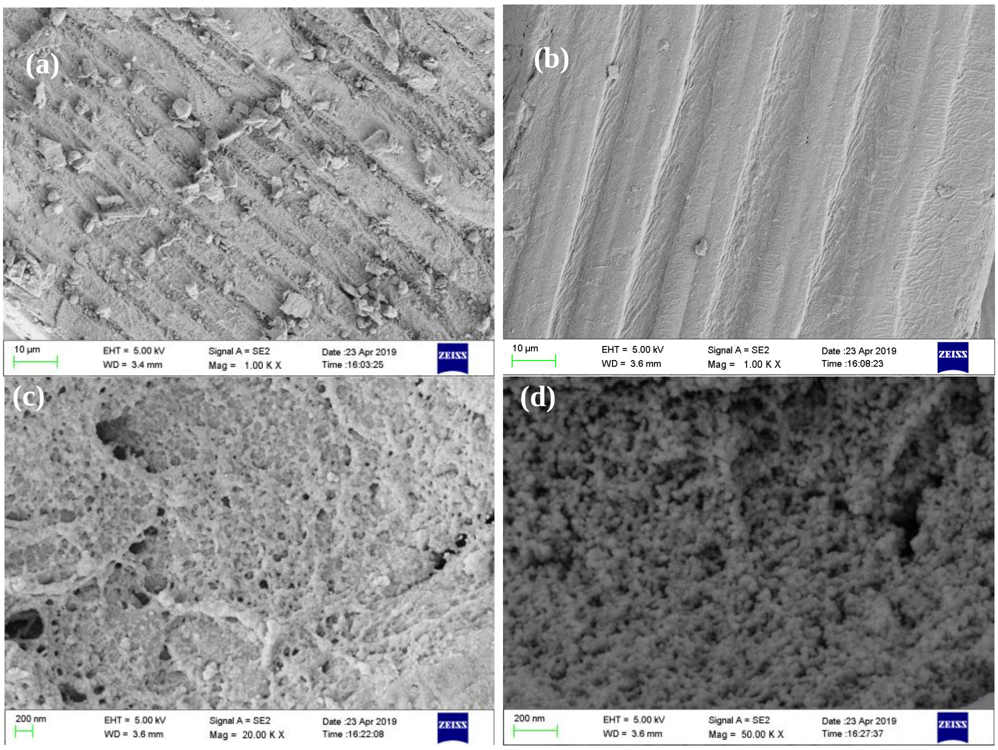

Figure 4. Scanning electron micrograph of garlic peel and HGAP-7 (a) garlic peel; (b) pickled garlic peel; (c) 20K magnification chart; (d) 50K magnification chart

In order to further explore the removal of endogenous minerals from garlic skin by pickling pretreatment, conduct EDS tests on garlic skin before and after pickling. Table 2 is the mass percentage of garlic peels obtained by EDS test, the pickling conditions are the best experimental conditions obtained above. After pickling garlic peel, the contents of C and N increased significantly. Compared with other mineral elements, the original content of Ca in garlic peel was the highest. And the removal effect is obvious, the removal rate is as high as 96.7%. It shows that the calcium salt in garlic peel can be dissolved in hydrochloric acid solution.

Table 2. Mass percentage of each element

Element	C	N	Mg	Al	K	Ca
garlic peel (%)	46.48	42.69	2.2	1.75	2.69	4.19
pickled garlic peel (%)	53.24	44.79	0.11	1.41	0.31	0.14
removal rate	*	*	95.0%	19.0%	88.4%	96.7%

3.2.3 Activated carbon crystallite structure

The influence of hydrochloric acid pretreatment on the graphitization degree of garlic skin-based activated carbon was tested by XDR and Raman. Figure 5 shows the XRD of HGAP-7 and GAP. As can be seen from figure, HGAP-7 has a diffraction peak at 2θ = 26 °, which corresponds to the characteristic diffraction peak of (002) crystal plane of activated carbon[22].

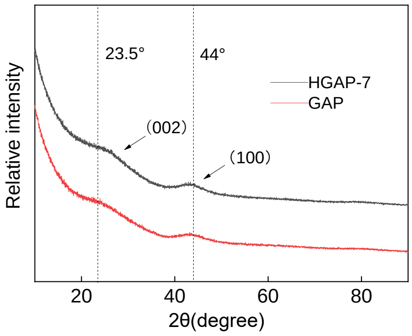

Figure 5. XRD diagram of GAP and HGAP-7

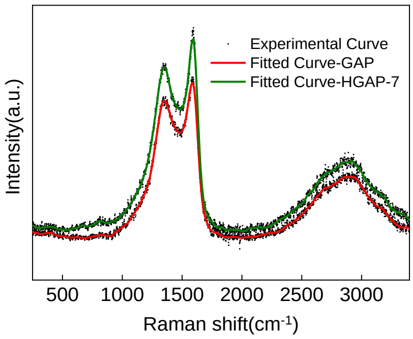

Figure 6. Raman spectrum of GAP and HGAP-7

However, the standard graphite peak 2θ = 23.5 °, so the characteristic diffraction peak of HGAP-7 showed a significant right shift. From the Prague formula: $2d\cdot\sin\theta=\lambda$, d_{002} decreases, it shows that the carbon layer spacing becomes smaller, proving that HGAP-7 has a certain degree of graphitization, but the crystallinity is poor, and it is an amorphous structure. GAP has a significant diffraction peak at 2θ = 24 °, but the characteristic diffraction peak shifts to the left compared to HGAP-7. According to the formula, it shows that the carbon layer spacing becomes larger compared to HGAP-7, the degree of graphitization is reduced. The two activated carbons have weaker graphite diffraction peaks at the (100) crystal plane of 2θ = 44 °, indicating that amorphous carbon is the main type of activated carbon[24].

According to Figure 6, HGAP-7 has a D-band peak near 1351 cm^{-1}, a G-band peak around 1600 cm^{-1}, and a 2D band peak around 2923 cm^{-1}. Amorphism can be expressed by the ratio of the peaks of D peak (defect and disorder) and G peak (graphite order), the larger the ratio, the lower the degree of order of the graphite material[25]. From the figure, the ratio of GAP is $I_D/I_G=0.9$, and the ratio of HGAP-7 is $I_D/I_G=0.88$, it is proved that HGAP-7 is more graphitized and more ordered than GAP. The peak in the 2D band reflects the number of graphite layers. The fewer the layers, the sharper the peak. HGAP-7 peak in the figure is steamed bread-shaped, not sharp, which proves that there is no single-layer graphite structure in HGAP-7. The analysis of the Raman test proves that the hydrochloric acid pre-pickling can effectively improve the orderliness of the activated carbon structure.

3.3. Electrochemical performance of garlic peel-based activated carbon electrode

3.3.1. Constant current charge-discharge characteristics of garlic peel-based activated carbon electrode

The calculation formula of the specific capacitance of the activated carbon electrode is[26]:

$$C_{\mathrm{p}} = \frac{4\mathrm{i}\Delta \mathrm{t}}{\mathrm{m a}\Delta V}$$

In the formula: Cp is the electrode mass specific capacitance, F/g; m is the mass of the double electrode, g; i is the charge and discharge current, A; α is the mass fraction of activated carbon on the electrode, %; Δ t is the time difference during charging, s; ΔV is the potential difference during charging, V.

In this research, calculate the specific capacitance according to the formula[27],HGAP-7 has a specific capacitance of 424.42 F/g at a current density of 1 A/g, which is better than most other biomass-based electrode materials(As shown in Table 3). Select HGAP-7 to explore its constant current charge and discharge characteristics under different current densities. As can be seen from Figures 7 (a) and (b), all curves exhibit a good isosceles triangle shape, and when the current density increases to 50 A/g, the charge-discharge curve still maintains good symmetry, indicating that the supercapacitor has good electric double layer capacitance properties. At the moment, when the supercapacitor changes from charging to discharging, there is almost no voltage drop, indicating that the equivalent series resistance of garlic peel-based activated carbon is small[28].

Figure 7 (c) is the specific capacitance of HGAP-7 and GAP at different current densities. As can be seen from the figure, as the current density increases, the specific capacitance of both gradually decreases, but HGAP-7 decayed significantly slower. When the current density is 50 A/g, with the current density of 1 A/g as the reference, the capacitance retention rates are 73.8% and 63%, respectively, with a significant difference. Hydrochloric acid pretreatment process can remove most of the endogenous minerals in garlic peel, improves the stability of garlic peel-based activated carbon skeleton. At larger current densities, the pore structure is less likely to collapse, thereby increasing its specific capacitance at high current densities. Compared with other biomass materials in Table 3, the pickled garlic skin-based activated carbon has better electrochemical performance.

Table 3. Electrochemical properties of precursors of different biomass materials

Raw materials	Activator	Electrolyte	Current density (A/g)	Specific capacity (F/g)	Ref
Onion	KOH	6 M KOH	0.5	180	[29]
Cicada slough	KOH	6 M KOH	1	274	[30]
Elm samara	KOH	6 M KOH	1	370	[31]
Stiff silkworm	KOH	6 M KOH	1	235	[32]
Chitosan	$KHCO_3$	1 M $ZnSO_4$	0.1	307.8	[33]
This work	KOH	6 M KOH	1	424.42	-

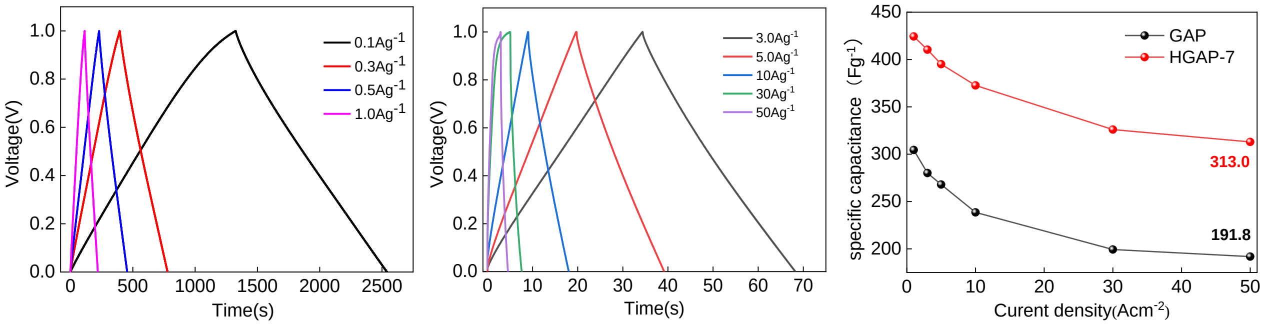

Figure 7. GCD curve and capacitor retention rate of garlic-based activated carbon (a) GCD curve of the HGAP-7 sample at current densities from 0.1 A/g to 1 A/g; (b) GCD curve of the HGAP-7 sample at current densities from 3 A/g to 50 A/g; (c) Specific capacitance of HGAP-7 and GAP at different current densities

3.3.2 Cyclic voltammetry characteristics of garlic peel-based activated carbon electrode

The ideal cyclic volt-ampere curve of the capacitor should be a standard rectangle, but in practice, due to the existence of internal resistance and other factors, the curve has a certain deviation. As can be seen from Figure 8, at different scan rates, the cyclic voltammograms all present an approximately rectangular shape. It has typical electric double-layer capacitance characteristics and no redox peak, the electric double-layer electrode fully provides the required capacity of the electrode. The scan rate is increased from 5 mV/s to 200 mV/s, still maintaining a good rectangular shape. When the scan rate is increased to 200 mV/s, the cyclic voltammetry characteristic curve still maintains a rectangular shape, which proves that it has excellent ion transport capability[34].

3.3.3 Impedance performance of garlic peel-based activated carbon electrode

The ideal AC impedance diagram of an electric double layer capacitor should be a straight line perpendicular to the X axis. Actually, due to the internal resistance between the electrode of the supercapacitor and the electrolyte, the AC impedance graph will appear semicircular in the high-frequency region[35]. As can be seen from Figure 9, the equivalent series resistance (ESR) is the intercept from the X axis, the ESR of HGAP-7 and GAP are 0.199 Ω and 0.316 Ω, and the equivalent series resistance of HGAP-7 is smaller. In the intermediate frequency region, the diffusion impedance of HGAP-7 and GAP deviates linearly by 45 °, and is close to the Y axis, indicating that the diffusion resistance is small. The hydrochloric acid pretreatment process removes garlic peel impurities, improves the pore structure of garlic peel-based activated carbon, improves the mesopore content and the stability of the carbon skeleton, and effectively reduces the internal resistance of the HGAP-7 electrode.

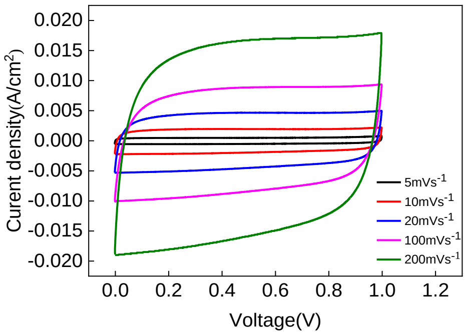

Figure 8. Cyclic voltammetry curves of HGAP-7 at different scan rates

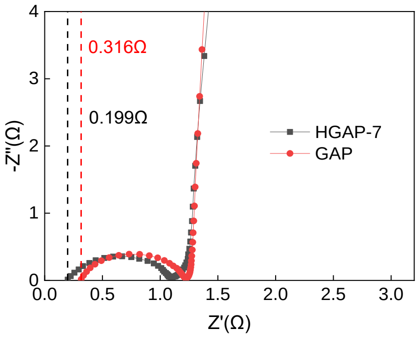

Figure 9. AC impedance diagram of GAP and HGAP-7

3.3.4 Cyclic stability of garlic peel-based activated carbon electrode

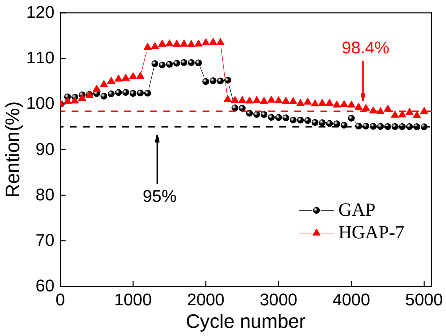

Figure 10. Cyclic performance of GAP and HGAP-7 at 5 A/g current density

To compare the long-cycle stability of supercapacitors with HGAP-7 and GAP as electrodes, at a current density of 5 A/g, the supercapacitors made by HGAP-7 and GAP were charged and discharged 5000 times with constant current. As shown in Figure 10, HGAP-7 capacitance attenuation is significantly weaker than GAP. After 5000 cycles, the capacitance retention rate was as high as 98.4%, and the GAP was only 95.0%. It shows that the carbon skeleton structure of HGAP-7 is more stable after hydrochloric acid pretreatment. HGAP-7 has a larger specific surface area and a more developed pore structure, and the cycle stability is improved.

4. CONCLUSION

Impurities such as endogenous minerals contained in garlic peel are not conducive to the formation of pores during the carbonization activation process. This study explored the optimal process conditions for hydrochloric acid pretreatment, garlic peel-based activated carbon with high specific surface area and large pore volume was prepared by removing endogenous minerals from garlic peel. After pretreated with a 1.0 mol L^{-1} hydrochloric acid solution at the water bath temperature of 60°C for 3 h, the precursor was carbonized at 600°C for 2 h and activated at. Finally, the optimized sample HGAP-7 has a specific surface area of 3325.2 m^2 g^{-1}, and the pore volume is 1.881 cm^3 g^{-1}. The supercapacitor assembled by it possesses a specific capacitance of 424.42 F g^{-1} at a current density of 1 A g^{-1}. When the current density is 50 A g^{-1}, the specific capacitance can still reach 313 F g^{-1}. After 5000 cycles at a current density of 5 A g^{-1}, the specific capacitance retention is as high as 98.4%. After the garlic peel was pretreated with hydrochloric acid, the cycle performance and the rate performance of the supercapacitors assembled by HGAP-7 electrodes both significantly improved. It proves that the existence of endogenous minerals has an inhibitory effect on the formation of well-developed pore structure derived from garlic peel, which determines the electrochemical performance of garlic peel-based activated carbon electrodes. Hydrochloric acid pretreatment can effectively improve the electrochemical performance of activated carbon.

ACKNOWLEDGEMENT

The authors would like to acknowledge funding support by the Natural Science Foundation of Shandong, China (ZR2017MEE010), and the Fundamental Research Funds of Shandong University (2016JC005).

References

1. S. Li, K. Han, P. Si, J. Li, C. Lu, *Int J Electrochem Sci*, 13 (2018) 1728.
2. Z. Teng, K. Han, J. Li, Y. Gao, M. Li, T. Ji, *Ultrason Sonochem*, 60 (2019) 104756.
3. A.G. Pandolfo and A.F. Hollenkamp, *J Power Sources*, 157 (2006) 11.
4. H. Wang, J. Varghese and L. Pilon, *Electrochim Acta*, 56 (2011) 6189.
5. L.L. Zhang and X.S. Zhao, *Chem Soc Rev,* 38 (2009) 2520.
6. K. Lota, I. Acznik, A. Sierczynska, and G. Lota, *Mater Lett*, 173 (2016) 72.
7. C. Zhong, Y. Deng, W. Hu, J. Qiao, L. Zhang, and J. Zhang, *Chem Soc Rev*, 44 (2015) 7484.
8. J. Zhou, Y. Huang, X. Cao, B. Ouyang, W. Sun, C. Tan, Y. Zhang, Q. Ma, S liang, Q. Yana, H. Zhang, *Nanoscale*, 7 (2015) 7035.
9. Y. Li, Y. Liu, W. Zhang, C. Guo, C. Chen, *Mater Lett*, 157 (2015) 273.
10. G. Zhao, Y. Li and G. Zhu, J. Shi, T. Lu, L. Pan, Acs *Sustain Chem Eng*, 7 (2019) 12052.
11. X. He, P. Ling, J. Qiu, M. Yu, X. Zhang, Y. Chang, and M. Zheng, *J Power Sources*, 240 (2013) 109.
12. B. Gu, X. Cao, L. Zhao, Y. Zhao, *Journal of Agro-Environment Science*, 36 (2017) 591.

13. K. Raveendran, A. Ganesh and K.C. Khilar, *Fuel,* 74 (1995) 1812
14. Z. Liang, B. Zhou, Y. Zou, *Journal of Fruit Science*, 29 (2012) 139.

15. L. Shi, S. Yu, F. Wang, and J. Wang, 96 (2012) 586.
16. L. Burhenne, J. Messmer, T. Aicher, and M. Laborie, *Journal of Analytical & Applied Pyrolysis*, 101 (2013) 177.
17. X. Wang, H. Chen, J. Wang, H. Yang, *Journal of Fuel Chemistry and Technology*, 36 (2008) 679.
18. Q. Sun, S. Yu, F. Wang, J. Wang, *Fuel*, 90 (2011) 1041.
19. Q. Zhang, K. Han, S. Li, M. Li, J. Li, and K. Ren, *Nanoscale*, 10 (2018) 2427.
20. P. Das, A. Ganesh and P. Wangikar, *Biomass Bioenerg*, 27 (2004) 445.
21. P. Kleszyk, P. Ratajczaka, P. Skowrona, J. Jagiellob, Q. Abbasa, E. Frąckowiaka, F. Béguina, *Carbon*, 81 (2015) 148.
22. C. Long, L. Jiang, X. Wu, Y. Jiang, D. Yang, C. Wang, T. Wei, Z. Fan, *Carbon*, 93 (2015) 412.
23. D. Wang, F. Li, H. Fang, M. Liu, G. Lu, H. Chen, *The journal of physical chemistry*. B, 110 (2006) 8570.
24. C. Wu, S. Yang, J. Cai, Q. Zhang, Y. Zhu, K. Zhang, *Acs Appl Mater Inter*, 8 (2016) 15288.
25. A.C. Ferrari, J.C. Meyer, V. Scardaci, C. Casiraghi, M. Lazzeri, F. Mauri, S. Piscanec, D. Jiang, K.S. Novoselov, S. Roth, A. K. Geim, *Phys Rev Lett*, 97 (2006) 187401.
26. D. Qu and H. Shi, *J Power Sources*, 74 (1998) 99.
27. X. Dong, X. Wang, J. Wang, H. Song, X. Li, L. Wang, M.B. Chan-Park, C.M. Li, and P. Chen, *Carbon*, 50 (2012) 4865.
28. Z. Hai, B. Lv, X. Yao, and W. Dong, *Mater Res Bull*, 50 (2014) 399.
29. J. Wang, P. Nie, B. Ding, S. Dong, X. Hao, H. Dou, and X. Zhang, *J Mater Chem* a, 5 (2017) 2411.
30. Y. Zhu, M. Chen, Y. Zhang, W. Zhao, and C. Wang, *Carbon*, 140 (2018) 404.
31. A. Uzi, Y. Shen, S. Kawi, A. Levy, and C. Wang, *Chem Eng J*, 355 (2019) 255.
32. J. Wang, L. Shen, Y. Xu, H. Dou, X. Zhang, *New J Chem*, 39 (2015) 9497.
33. H. Wang, M. Wang and Y. Tang, *Energy Storage Materials*, 13 (2018) 1.

34. C. Long,L. Jiang, X. Wu, Y. Jiang, D. Yang, C. Wang, T. Wei, Z. Fan, *Carbon*, 93 (2015) 412.
35. H. Wang, Z. Xu, A. Kohandehghan, Z. Li, K. Cui, X. Tan, T. Stephenson, C. King, C.Holt, B. Olsen, J. Tak, D. Harfield, A. Anyia, D. Mitlin. *Acs Nano*, 7 (2013) 5131.